Theory of the correlated-electron semiconductor $Ce_3Bi_4Pt_3$

S. H. Liu
Department of Physics, University of California, San Diego, La Jolla, California 92093-03219
(Received 3 December 1998; revised manuscript received 10 May 1999)

There is considerable experimental evidence that the material $Ce_3Bi_4Pt_3$ has a narrow conduction band. Assuming this band to be *d*, we show that $d-f$ interactions, hybridization plus Coulomb interaction, can stabilize a two-electron localized state with mixed *d* and *f* characters below the edge of the conduction band. The state is in a singlet spin configuration, and both $4f$ and $5d$ electrons of the Ce atom may enter this level. A nonmagnetic insulating ground state is formed when every Ce site is populated by this two-electron localized state. At finite temperatures one electron is readily excited into the conduction band to provide conductivity, leaving the other in a one-electron local level to produce magnetic moment. The conduction electrons are scattered off the Coulomb potential of the local electron, and at the same time, screen the potential in a temperature-dependent manner. The combined effects explain the unusual temperature dependence of the resistivity and the Hall mobility. The model describes the inelastic neutron scattering cross section, and predicts an unusual neutron magnetic form factor. A large and temperature-dependent dielectric constant is predicted. [S0163-1829(99)09843-4]

I. INTRODUCTION

The compound $Ce_3Bi_4Pt_3$ is the most thoroughly studied member of a class of solids commonly known as ''Kondo insulators.''[1,2] The following is a summary of its basic properties. The electrical resistivity rises with decreasing temperature, by three orders of magnitude in a good sample between room and low temperatures.[2,3] The data establish that the material is an insulator, but a plot of $\ln\rho$ versus temperature does not yield a clear thermal activation behavior. Also, there is no evidence of $\ln T$ temperature dependence nor hint of low-temperature saturation characteristic of Kondo impurities. The Hall mobility is negative, which indicates electron conduction. The data exhibit a sharp and sample-dependent peak around 10 K.[3] The magnetic susceptibility follows a Curie-Weiss law above approximately 150 K. It peaks at 80 K, then falls to a low-temperature limiting value of approximately one-half of the peak value after a sample dependent, low-temperature Curie tail is subtracted.[4] The ratio of peak to low-temperature values of the susceptibility is too high compared with what is predicted for Kondo impurities. The specific heat γ is low and sample dependent.[3,5] The authors concluded that γ vanishes for the pure material. Although the full electronic contribution to the specific heat curve has not been measured, Kwei *et al.*[6] have deduced a semiquantitative result from the thermal expansion data and the Grüneisen parameter. Their curve has the shape of a Schottky anomaly peaked at 50 K, and the entropy under the curve is roughly $R\ln 6$ per mole. The position of the peak is consistent with an energy gap in the electronic excitation spectrum of approximately 100-160 K.

Inelastic neutron scattering on a powdered single-crystal sample of $Ce_3Bi_4Pt_3$ has provided evidence of an energy gap in the electronic spectrum at small scattering angles.[7,8] At 2 K the magnetic scattering intensity vanishes for energy transfers smaller than 12 meV ($\simeq$140 K), rises sharply between 12 and 20 meV, then falls off steadly to zero around 65 meV ($\simeq$780 K). Above 100 K the gap structure gradually disappears. No unusual magnetic scattering is seen at large scattering angles because the scattering intensity has the same energy dependence as $La_3Bi_4Pt_3$. In summary, the data support an energy gap of approximately 140 K in the low-momentum region of the Brillouin zone. The size of the gap is in good agreement with the value estimated from anomalous thermal expansion by Kwei *et al.*[6]

The origin of the gap has been attributed by Fisk *et al.*,[1] to the hybridization gap, i.e., the gap in the band structure of a periodic spin fluctuation system in the low-temperature coherent state.[11,12] There is an inconsistency in this picture, however, because Kwei *et al.* pointed out that the hybridization gap is an *indirect* gap, i.e., the gap between the upper band at the zone center and the lower band at the zone boundary. The direct gap at the band-crossing point is expected to be much larger. Accordingly, they predicted that the gap could be seen by neutron magnetic scattering at large scattering angles.[6] The experiment of Severing *et al.* made it clear that the magnetic gap is identical to the thermodynamic gap, and is not an indirect gap.[7,8] Thus, the hybridization gap picture and the associated spin fluctuation theory are in conflict with experimental findings.

The best developed theory along this vein was proposed by Duan *et al.*[13] They studied the Coulomb attraction between *f* holes and conduction electrons and suggested that the low-temperature phase is an excitonic insulator state. The condensate has *p*-wave symmetry, and coupling of the excitons to the lattice deformation leads to a ferroelastic transition.[14,15] The authors were able to fit the temperature dependence of the magnetic susceptibility above 120 K, and to explain the observed correlation between the susceptibility and the lattice expansion.[3] A phase transition is predicted such that the elastic constant makes a jump and the phonons show anomalous behavior at the transition. On the negative side, the theory predicts an indirect gap of 44 K, in disagreement with neutron scattering experiments. There is no sign

of a phase transition, ferroelectric or otherwise, in thermodynamic or transport data up to 350 K. Also, the calculated susceptibility does not fit the experimental data at low temperatures, and the discrepancy is beyond what can be attributed to impurity effect.

Two independent experiments have given evidence that the material has a narrow conduction band. Reyes *et al.*[4] demonstrated that, in order to fit their nuclear-spin relaxation data, they need to model the electronic structure of this material by a conduction band whose width is 1200 K, and a valence band of width 100 K, separated by an energy gap of 190 K. In addition, the inelastic neutron scattering at low temperatures measures the excitation of an electron from the valence band to the conduction band. The width of the conduction band deduced from the data is around 600 K.[7,8] A third set of experiments, the doping experiments reported by Canfield *et al.* shed further light on the existence and the character of the narrow band.[9] In these experiments one replaces Ce partially by La in $Ce_3Bi_4Pt_3$. It was found that La acts like a donor even though it has one fewer electron than Ce, and La doping causes γ to increase while leaving the gap almost unchanged. This behavior hints that the d electron in Ce is tied down by the f electron in a correlated pair which is broken up on La sites because there is no f electron. That the gap remain unaffected reflects the local nature of the correlated $d-f$ pair. The d electron on La goes into the conduction band to provided electron conduction and specific heat γ. The γ values for various amounts of doping, ranging from 20 to 150 mJ/mole K^2, indicates that the width of the conduction band is a few hundred K, in agreement with nuclear-spin relaxation and neutron scattering experiments. The fact that La d electrons readily enter the narrow band may be regarded as indication that the band is derived from Ce d. It should be noted that the occurance of narrow conduction band is not unique to f electron systems. The material LiV_2O_4 has specific heat $\gamma = 420$ mJ/mol K^2, which is of heavy fermion scale, but has no f electron in its chemical components.[10]

While most workers in this field regard the narrow conduction band as the leading challenge, we feel that it may be profitable to explore a new avenue. We propose to take the narrow conduction band as given and explore its consequences. In this paper, we use the well-known periodic Anderson model to show that, when the width of the conduction band is less than the strength of the hybridization potential, the $d-f$ hybridization problem has a novel solution. The solution consists of a local spin-compensated two-electron state at every Ce site below the conduction-band edge. Both $4f$ and $5d$ electrons of the Ce atom fall into the local state to create a nonmagnetic insulating ground state. At finite temperatures some singlet pairs break up, sending one electron into the conduction band and the other electron into an unpaired one-electron local state. We will demonstrate that this model describes the observed properties of the system. As ways to verify the model assumptions, we have predicted an anomalous neutron scattering form factor and a large and temperature sensitive dielectric constant, both can be readily checked experimentally.

II. THEORY

The bulk of the theory is developed in this Section. Section II A shows that a one-electron local state can be stabilized in the narrow band system. This state is relevant to the first excited state, but is mathematically much simpler compared with the two-electron local state, which is the building block of the ground state. Derivation of the two-electron local state follows in Sec. II B. Section II C investigates the conduction band states. Section II D summarizes our findings and works out the consequences of this theory.

A. The one-electron local state

The following Hamiltonian summarizes all interactions that are relevant in the system ($\hbar = k_B = 1$)

$$H = \sum_{\vec{k}\sigma} \epsilon_k c^\dagger_{\vec{k}\sigma} c_{\vec{k}\sigma} + \sum_{j\sigma} \epsilon_f f^\dagger_{j\sigma} f_{j\sigma} + \frac{1}{\sqrt{N}} \times \sum_{\vec{k},j\sigma} (V_{\vec{k}} f^\dagger_{j\sigma} c_{\vec{k}\sigma} e^{i\vec{k}\cdot\vec{R}_j} + \text{H.c.}) + U_{ff} \times \sum_j f^\dagger_{j+} f_{j+} f^\dagger_{j-} f_{j-} + U_{dd} \sum_j c^\dagger_{j+} c_{j+} c^\dagger_{j-} c_{j-} + U_{df} \sum_{j\sigma} c^\dagger_{j\sigma} c_{j\sigma} \left(\sum_{\sigma'} f^\dagger_{j\sigma'} f_{j\sigma'} - 1 \right), \quad (1)$$

where

$$c_{j\sigma} = \frac{1}{\sqrt{N}} \sum_{\vec{k}} c_{\vec{k}\sigma} e^{i\vec{k}\cdot\vec{R}_j}. \quad (2)$$

The first term on the right-hand-side of Eq. (1) is the energy of the conduction band with $0 \leqslant \epsilon_k \leqslant W$, W being the band width. There is one $5d$ electron for each Ce atom. The second term is the energy of the localized f levels. For simplicity, we consider only a Kramers doublet of f levels. The V term represents the $d-f$ hybridization interaction, N is the number of Ce sites in the sample. The last three terms represent various Coulomb interactions. The term involving U_{ff} denotes the Coulomb repulsion between two f electrons with opposite spins on the same site. It is so strong that it prevents the f level from more than singly occupied. The U_{dd} term is the Coulomb interaction between two electrons in the conduction band. This may be important because the band is narrow. The U_{df} term represents the attractive Coulomb interaction between an f hole and a conduction electron on the same site. It has been invoked by Falicov and coworkers to explain the α to γ phase transition of Ce,[16,17] and by the present author for the crossover from coherent to incoherent states in heavy fermion materials.[18]

In the first step of our discussion, we consider the $d-f$ hybridization problem at the site situated at $\vec{R}_j$ in the ground state. The effective Hamiltonian is

$$H_j=\sum_{\vec{k}\sigma}\epsilon_k c^\dagger_{\vec{k}\sigma}c_{\vec{k}\sigma}+\sum_\sigma \epsilon_f f^\dagger_{j\sigma}f_{j\sigma}+\frac{1}{\sqrt{N}}\times\sum_{\vec{k}',\sigma}(V_{\vec{k}}f^\dagger_{j\sigma}c_{\vec{k}\sigma}e^{i\vec{k}\cdot\vec{R}_j}+\text{H.c.})+U_{ff}f^\dagger_{j+}f_{j+}f^\dagger_{j-}f_{j-}+U_{dd}c^\dagger_{j+}c_{j+}c^\dagger_{j-}c_{j-}+U_{df}\sum_\sigma c^\dagger_{j\sigma}c_{j\sigma}\left(\sum_{\sigma'}f^\dagger_{j\sigma'}f_{j\sigma'}-1\right). \tag{3}$$

The wave function of the local one-electron state is assumed to be

$$\phi_{j\sigma}=af_{j\sigma}+\sum_{\vec{k}} b_{\vec{k}}c_{\vec{k}\sigma}e^{i\vec{k}\cdot\vec{R}_j}, \tag{4}$$

which satisfies the Schrödinger equation $[\phi_{j\sigma},H_j]=\omega_1\phi_{j\sigma}$. For the left-hand side of the equation we need to work out the commutators

$$[f_{j\sigma},H_j]=\epsilon_f f_{j\sigma}+\frac{1}{\sqrt{N}}\sum_{\vec{k}} V_{\vec{k}}c_{\vec{k}\sigma}e^{i\vec{k}\cdot\vec{R}_j}+U_{ff}f_{j\sigma}f^\dagger_{j,-\sigma}f_{j,-\sigma}+U_{df}\sum_{\sigma'} c^\dagger_{j\sigma'}c_{j\sigma'}f_{j\sigma}, \tag{5}$$

and

$$[c_{\vec{k}\sigma},H_j]=\epsilon_k c_{\vec{k}\sigma}+\frac{1}{\sqrt{N}}V^*_{\vec{k}}f_{j\sigma}e^{-i\vec{k}\cdot\vec{R}_j}+\frac{U_{dd}}{\sqrt{N}}c_{j\sigma}c^\dagger_{j,-\sigma}c_{j,-\sigma}e^{-i\vec{k}\cdot\vec{R}_j}+\frac{U_{df}}{\sqrt{N}}c_{j\sigma}\left(\sum_{\sigma'}f^\dagger_{\sigma'}f_{\sigma'}-1\right)e^{-i\vec{k}\cdot\vec{R}_j}. \tag{6}$$

The effects of the Coulomb interaction terms are calculated according to the occupation of each configuration in the trial wave function. For instance, the a term, which has one f electron, the U_{ff} and U_{df} terms are inoperative. On the other hand, the U_{df} is important in the $b_{\vec{k}}$ terms in the wave function, while U_{dd} is inconsequential. Putting the results into the Schrödinger equation and equating like terms, we obtain

$$a(\epsilon_f-\omega_1)+\frac{1}{\sqrt{N}}\sum_{\vec{k}} b_{\vec{k}}V^*_{\vec{k}}=0, \tag{7}$$

and

$$b_{\vec{k}}(\epsilon_k-\omega_1)-\frac{U_{df}}{N}\sum_{\vec{k}'} b_{\vec{k}'}+a\frac{V_{\vec{k}}}{\sqrt{N}}=0. \tag{8}$$

We solve for a from Eq. (7) and substitute the result into Eq. (8) to obtain

$$b_{\vec{k}}(\epsilon_k-\omega_1)=\frac{1}{N}\sum_{\vec{k}'} b_{\vec{k}'}\left\{\frac{V_{\vec{k}}V^*_{\vec{k}'}}{\epsilon_f-\omega_1}+U_{df}\right\}. \tag{9}$$

The solution of the integral equation for $b_{\vec{k}}$, Eq. (9), requires knowledge of the $\vec{k}$ dependence of the hybridization potential $V_{\vec{k}}$.

While many authors consider the momentum dependence of hybridization potential unimportant, Duan *et al.* argued that $V_{\vec{k}}$ should be an odd function of $\vec{k}$, and this property leads to interesting physical consequences.[13] In this paper we will investigate the nature of the solution by considering a more general $V_{\vec{k}}$ which has an even part and an odd part in $\vec{k}$, i.e. $V_{\vec{k}}=V_0+V_1\hat{k}$, where $\hat{k}=\vec{k}/|\vec{k}|$. To simplify the algebra we treat both V_0 and V_1 as independent of $\vec{k}$. The solution for $b_{\vec{k}}$ has the form $b_{\vec{k}}=b_0(\vec{k})+b_1(\vec{k})\hat{k}$, where b_0,b_1 are both even in $\vec{k}$. Putting into Eq. (9) and separating even and odd parts in $\vec{k}$, we obtain the following coupled equations:

$$b_0(\epsilon_k-\omega_1)=\frac{(\langle b_0\rangle V^*_0+\langle b_1\rangle V^*_1)V_0}{\epsilon_f-\omega_1}+\langle b_0\rangle U_{df}, \tag{10}$$

and

$$b_1(\epsilon_k-\omega_1)=\frac{(\langle b_0\rangle V^*_0+\langle b_1\rangle V^*_1)V_1}{\epsilon_f-\omega_1}. \tag{11}$$

In the above equation, $\langle b_0\rangle=N^{-1}\Sigma_{\vec{k}}b_0(\vec{k})$, and similarly for $\langle b_1\rangle$. The equations are closed by dividing both sides by $\epsilon_k-\omega_1$ and summing over $\vec{k}$. In general we expect $U_{df}\gg|V|$, so we find from the above equations that $b_0\gg b_1$. Once b_1 is ignored, the equation for ω_1 becomes quite simple:

$$1=\frac{1}{N}\sum_{\vec{k}}\frac{1}{\epsilon_k-\omega_1}\left\{\frac{V_0^2}{\epsilon_f-\omega_1}+U_{df}\right\}. \tag{12}$$

In the narrow band limit we approximate

$$\frac{1}{N}\sum_{\vec{k}}\frac{1}{\epsilon_k-\omega_1}=\frac{1}{\langle\epsilon\rangle-\omega_1},$$

where $\langle\epsilon\rangle=\int D(\epsilon)\epsilon d\epsilon$, and $D(\epsilon)$ is the density of states of the conduction band per Ce atom per spin. Then ω_1 is solved from a quadratic equation whose lower root is

$$\omega_1=\tfrac{1}{2}(\epsilon_f+\langle\epsilon\rangle-U_{df})-\tfrac{1}{2}\sqrt{(\epsilon_f-\langle\epsilon\rangle+U_{df})^2+4V_0^2}. \tag{13}$$

There is strong mixing of d and f wave function if $|\epsilon_f-\langle\epsilon\rangle+U_{df}|\simeq V_0$, and only the even part of $V_{\vec{k}}$ is effective.

The wave function of the one-electron local state is found to be

$$\phi_{j\sigma}=af_{j\sigma}-bc_{j\sigma}, \tag{14}$$

where

$$a^2=\left\{1+\frac{V_0^2}{(\langle\epsilon\rangle-U_{df}-\omega_1)^2}\right\}^{-1}, \tag{15}$$

and $b^2=1-a^2$. The quantities a^2,b^2 measure the f and d content of the local level respectively.

B. Two-electron local state

We now investigate the two-electron local state with the pair in spin-singlet configuration. The algebra is substantially parallel to the one-electron problem, only more complicated. We choose the following trial wave function for the two-electron state:

$$\Phi_j=\sum_{\vec{k}}\ \alpha_{\vec{k}}(f_{j+}c_{\vec{k}-}+c_{\vec{k}+}f_{j-})e^{i\vec{k}\cdot\vec{R}_j}+\sum_{\vec{k}\vec{k}'}\ \beta_{\vec{k}\vec{k}'}c_{\vec{k}+}c_{\vec{k}-}e^{i(\vec{k}+\vec{k}')\cdot\vec{R}_j}, \tag{16}$$

which satisfies the Schrödinger equation $[\Phi_j,H_j]=\omega_0\Phi_j$. In the wave function in Eq. (16) the configuration with doubly occupied f level is explicitly left out on account of the large Coulomb repulsion U_{ff}. The evaluation of the commutator in the Schrödinger equation involves tedious algebra. Among the resulting terms we discard all doubly occupied f terms for the same reason that they are not included in the trial wave function. The Coulomb interaction effects are calculated according to the occupation of each configuration. For instance, the $\alpha_{\vec{k}}$ terms, which have one f electron, the U_{df} term is inoperative. Also, the U_{dd} term has no effect because there is no more than one d electron. On the other hand, both U_{df} and U_{dd} are important in $\beta_{\vec{k}\vec{k}'}$ terms in the wave function. In this manner, we obtain the following equations for the coefficients:

$$\alpha_{\vec{k}}(\epsilon_f+\epsilon_k)+\sum_{\vec{k}'}\ \beta_{\vec{k}'\vec{k}}\frac{V^*_{\vec{k}'}}{\sqrt{N}}=\alpha_{\vec{k}}\omega_0. \tag{17}$$

$$\alpha_{\vec{k}}\frac{V_{\vec{k}'}}{\sqrt{N}}+\alpha_{\vec{k}'}\frac{V_{\vec{k}}}{\sqrt{N}}+\beta_{\vec{k}\vec{k}'}(\epsilon_k+\epsilon_{k'})+\frac{U_{dd}}{N}\times\sum_{\vec{k}''}\ \beta_{\vec{k}\vec{k}''}-\frac{U_{df}}{N}\sum_{\vec{k}''}\ (\beta_{\vec{k}\vec{k}''}+\beta_{\vec{k}''\vec{k}'})=\beta_{\vec{k}\vec{k}'}\omega_0. \tag{18}$$

We solve for $\alpha_{\vec{k}}$ from Eq. (17), substitute the result into Eq. (18), and sum over $\vec{k},\vec{k}'$ to obtain

$$\sum_{\vec{k}\vec{k}'}\ \beta_{\vec{k}\vec{k}'}=\sum_{\vec{k}\vec{k}'}\ \frac{1}{\epsilon_k+\epsilon_{k'}-\omega_0}\Bigg[-\frac{U_{dd}}{N}\sum_{\vec{k}''}\ \beta_{\vec{k}\vec{k}''}+\frac{U_{df}}{N}\sum_{\vec{k}''}\ (\beta_{\vec{k}\vec{k}''}+\beta_{\vec{k}''\vec{k}'})+\frac{1}{N}\sum_{\vec{k}''}\ \beta_{\vec{k}''\vec{k}}\frac{V_{\vec{k}'}V^*_{\vec{k}''}}{\epsilon_f+\epsilon_k-\omega_0}+\frac{1}{N}\sum_{\vec{k}''}\ \beta_{\vec{k}''\vec{k}'}\frac{V_{\vec{k}}V^*_{\vec{k}''}}{\epsilon_f+\epsilon_{k'}-\omega_0}\Bigg]. \tag{19}$$

This is the eigenvalue equation for the energy ω_0.

In the narrow band limit both ϵ_k and $\epsilon_{k'}$ can be replaced by the average band energy $\langle\epsilon\rangle$. Just like the one-electron case, we find that only the even part of $V_{\vec{k}}$ participates in hybridization when the Coulomb interactions U_{dd} and U_{df} are present. Accordingly, we replace $V_{\vec{k}}$ by V_0 to obtain

$$\sum_{\vec{k}\vec{k}'}\ \beta_{\vec{k}\vec{k}'}=\sum_{\vec{k}\vec{k}'}\ \beta_{\vec{k}\vec{k}'}\frac{1}{2\langle\epsilon\rangle-\omega_0}\times\left\{2U_{df}-U_{dd}+\frac{2V_0^2}{\epsilon_f+\langle\epsilon\rangle-\omega_0}\right\}. \tag{20}$$

The energy ω_0 of the two-electron level is solved from a quadratic equation whose lower root is

$$\omega_0=\frac{1}{2}(\epsilon_f+3\langle\epsilon\rangle+U_{dd}-2U_{df})-\frac{1}{2}\sqrt{(\epsilon_f-\langle\epsilon\rangle-U_{dd}+2U_{df})^2+8V_0^2}. \tag{21}$$

The $d-f$ hybridization effect is important provided that $|\epsilon_f-\langle\epsilon\rangle-U_{dd}+2U_{df}|\simeq\sqrt{2}V_0$.

The wave function of the two-electron state can be calculated from the equations of its coefficients. We find

$$\Phi_j=\alpha[f_{j+}c_{j-}+c_{j+}f_{j-}]-\beta c_{j+}c_{j-}, \tag{22}$$

where $c_{j\sigma}$ was defined in Eq. (2),

$$\alpha=\frac{V_0}{\sqrt{(\epsilon_f+\langle\epsilon\rangle-\omega_0)^2+2V_0^2}}, \tag{23}$$

and $\beta^2=1-2\alpha^2$. The occupation of the f level is $2\alpha^2$, while the occupation of the localized d level is $2(1-\alpha^2)$. Under suitable conductions to be discussed later, the ground state is a lattice of occupied two-electron states with no electron in the conduction band.

C. The conduction band

The nature of the now-empty conduction band is also important to our discussion. We go back to the full Hamiltonian H in Eq. (1) and study the commutators

$$[c_{\vec{k}\sigma},H]=\epsilon_k c_{\vec{k}\sigma}+V^*_{\vec{k}}f_{\vec{k}\sigma}+\frac{U_{dd}}{\sqrt{N}}\sum_j\ c_{j\sigma}c^\dagger_{j,-\sigma}c_{j,-\sigma}e^{-i\vec{k}\cdot\vec{R}_j}+\frac{U_{df}}{\sqrt{N}}\sum_{\vec{k}'}\ c_{j\sigma}\left(\sum_{j\sigma'}\ f^\dagger_{j\sigma'}f_{j\sigma'}-1\right)e^{-i\vec{k}\cdot\vec{R}_j}, \tag{24}$$

and

$$[f_{\vec{k}\sigma},H]=\epsilon_f f_{\vec{k}\sigma}+V_{\vec{k}}c_{\vec{k}\sigma}+\frac{U_{ff}}{\sqrt{N}}\sum_j\ f_{j\sigma}f^\dagger_{j,-\sigma}f_{j,-\sigma}e^{-i\vec{k}\cdot\vec{R}_j}+\frac{U_{df}}{\sqrt{N}}\sum_{j\sigma'}\ c^\dagger_{j\sigma'}c_{j\sigma'}f_{j\sigma}e^{-i\vec{k}\cdot R_j}. \tag{25}$$

Next, we replace the electron occupation operators by their ground-state expectation values to obtain

$$[c_{\vec{k}\sigma},H]=[\epsilon_k+U_{dd}(1-\alpha^2)-U_{df}\beta^2)]c_{\vec{k}\sigma}+V^*_{\vec{k}}f_{\vec{k}\sigma}, \tag{26}$$

and

$$[f_{\vec{k}\sigma},H]=[\epsilon_f+U_{ff}\alpha^2+2U_{df}(1-\alpha^2)]f_{\vec{k}\sigma}+V_{\vec{k}}c_{\vec{k}\sigma}. \tag{27}$$

Since U_{ff} is overwhelmingly large, the renormalized f level is high so that hybridization with d becomes impossible. The band remains d, with renormalized band energy solved from Eq. (26):

$$\omega_k = \epsilon_k + \epsilon_b, \tag{28}$$

where $\epsilon_b = U_{dd}(1-\alpha^2) - U_{df}\beta^2$. The band is simply shifted from the original position by ϵ_b.

The wave functions of the renormalized band must change in order to satisfy the Schrödinger equation with the added potential. We represent the operators of the new states by $\tilde{c}_{k\sigma}$, and for our purpose we only need to note that they are d states. We also argue that they are orthogonal to the local states for the following reason. In the impurity model where there is only one Ce site, the scattering states are orthogonal to the bound state. We expect the orthogonality to hold in the impurity lattice model as long as the local pair wave functions on different sites do not overlap, as obtained in the narrow band limit.

In the first excited state a two-electron state is broken up into a one-electron state plus one electron in the band. If we denote the excited site by j, then from Eq. (27) we find a local scattering potential for the band electron resulting from the change of local population

$$V_{coul} = U_{dd}(b^2 - 1 + \alpha^2) + U_{df}(a^2 - 2\alpha^2), \tag{29}$$

which is located at the site j. This added potential has no effect on the band energy, but scatters the band electrons and contributes to resistivity at finite temperatures. Other consequences of the model will be discussed next.

D. Physical properties of the model

The insulating state exists if the two-electron state is stable against spontaneous decay into a one-electron state and a band state. This requires

$$\Delta = \omega_1 + \epsilon_b - \omega_0 > 0. \tag{30}$$

The quantity Δ plays the role of the energy gap. The model has too large a parameter space to make a precise mapping of the stability region practical. In Appendix A we show that a neighborhood in the space exists such that a semiconductor with an energy gap of the right order of magnitude is stable. From here on Δ will be treated as a fitting parameter.

The energy difference between the ground state and the first excited state spans a continuum from Δ to $\Delta + W$, where W is the width of the conduction band. It would take much higher energy to empty out the one-electron state, so we need only to include singly and doubly occupied sites in solving the statistical mechanical problem. Let N_1 be the number of excited sites, then

$$n_1 \equiv \frac{N_1}{N} = \frac{1}{e^{(\mu-\Delta)/T}+1}, \tag{31}$$

where μ is the Fermi energy and T is the temperature. The number of electrons in the conduction band must be equal to the number of excited sites, so

$$n_1 = 2\int_0^W D(\epsilon) f(\epsilon) d\epsilon, \tag{32}$$

and $f(\epsilon) = [e^{(\epsilon-\mu)/T}+1]^{-1}$. Equations (31) and (32) solve for both N_1 and μ. The internal energy of the system is

$$E = \omega_0 N + \Delta N_1 + 2N\int_0^W D(\epsilon) f(\epsilon)\epsilon d\epsilon. \tag{33}$$

The electronic contribution to the specific heat is calculated from differenting the internal energy E.

The magnetic susceptibility consists of three contributions. At zero temperature the only nonzero contribution is a Van Vleck or orbital term involving virtual transitions between the ground state and the continuum of first excited states:[19]

$$\chi_{vv} = 4\mu_{vv}^2 \int_0^W \frac{D(\epsilon)[1 - n_1 - f(\epsilon)]d\epsilon}{\Delta + \epsilon}, \tag{34}$$

where μ_{vv} is effective magnetic moment for the Van Vleck susceptibility. In Appendix B, we show that $\mu_{vv} = b(\alpha + \beta)\mu_B$, where μ_B is the Bohr magneton. At elevated temperatures two more terms emerge. As the conduction band is populated, a Pauli term appears

$$\chi_p = \frac{2\mu_B^2}{T}\int_0^W D(\epsilon) f(\epsilon)[1 - f(\epsilon)]d\epsilon. \tag{35}$$

The singly occupied sites now contribute to a Curie susceptibility

$$\chi_c = \frac{\mu_c^2 n_1}{T}, \tag{36}$$

where μ_c is the effective magnetic moment of the Curie susceptibility. In Appendix B, we deduce that $\mu_c = a^2\mu_f + b^2\mu_B$, where μ_f is the magnetic moment of the f electron.

Transport properties for this material are subtle. Simple theory of electron conduction gives the resistivity $\rho = m/ne^2\tau$, where m is the carrier mass, e is the electron charge, n is the carriers density, and τ is the scattering time. We showed earlier that the carrier density n is equal to the density of singly occupied sites n_1, which is the number of scatterers. If the scattering mechanism is magnetic in origin, as is commonly assumed, the scattering cross section would be independent of the kinetic energy of the carriers so that the product $n\tau$ is temperature independent. This type of theory is incapable of explaining the observed strong temperature dependence of the resistivity. We will show that a model based on Coulomb scattering gives the complex temperature-dependent scattering cross section that explains both the resistivity and the Hall mobility.

Each singly occupied site is a scattering site in an otherwise periodic potential. The potential originates from the V_{coul} term in Eq. (29), but in a semiconductor we must consider screening of the Coulomb interaction by electrons in the conduction band. For a parabolic band the inverse scattering time for a screened Coulomb scatterer is[20]

$$\frac{1}{\tau(\epsilon)} \propto \frac{N_c}{\epsilon^{3/2}}\int_0^1 \frac{z^2 dz}{(z^2 + \lambda^2\hbar^2/8m\epsilon)^2}, \tag{37}$$

where N_c is the density of Coulomb scatters, λ is the inverse screening length, and a number of fundamental parameters

are lumped into the proportionality constant. In our theory, $N_c = N_i + n_1$, where N_i is the density of impurities. The inverse screening length is a function of the conduction band occupation[21]

$$\lambda^2 = \frac{4\pi e^2}{\Omega_0 T}\int_0^W D(\epsilon) f(\epsilon)[1-f(\epsilon)]d\epsilon, \tag{38}$$

where Ω_0 is the crystal volume per Ce atom. The expressions for transport coefficients are more complex due to the energy dependence of τ.[22] We can write the resistivity as

$$\rho = \frac{mc}{ne^2}\frac{\langle\epsilon\rangle}{\langle\epsilon\tau\rangle}, \tag{39}$$

where

$$\langle O(\epsilon)\rangle = \int_0^W O(\epsilon) D(\epsilon) f(\epsilon)[1-f(\epsilon)]d\epsilon,$$

and the Hall mobility

$$\mu_H = \frac{e}{mc}\frac{\langle\epsilon\tau^2\rangle}{\langle\epsilon\tau\rangle}, \tag{40}$$

where c is the speed of light. Although we will use a more general band structure later, we can already deduce some qualitative results from the formulas above. The product $n\langle\tau\rangle$ vanishes at low temperatures because λ tends to zero, causing the resistivity to diverge. On the other hand, $\langle\tau\rangle$ itself diverges if $N_i = 0$, but vanishes when $N_i > 0$. This causes the Hall mobility to rise below 100 K but bends over around 10 K for a real sample. How the theory fits the actual data will be discussed in the next Section. The scattering between quasiparticles, another manifestation of U_{dd}, also contributes to the resistivity. This contribution has the same temperature dependence as the V_{coul} contribution, because the density of scatterers is the same as the density of carriers and the Coulomb interaction between pairs of conduction electrons is screened the same way as in Eqs. (37) and (38).

The inelastic neutron scattering cross section $S(\vec{Q},\omega)$ is related to the imaginary part of the dynamical susceptibility:[7]

$$S(\vec{Q},\omega) \propto \frac{\chi''(\vec{Q},\omega)}{1-e^{-\omega/T}}. \tag{41}$$

For small scattering angles we take the limit $\vec{Q}\to 0$. There are three contributions to the neutron scattering cross-section, in exact correspondence with the three terms in the static susceptibilty. The Van Vleck term comes from real transition between the ground state and the first excited states

$$\chi''_{vv}(0,\omega) = 4\pi\mu_{vv}^2 D(\omega-\Delta)[1-n_1-f(\omega-\Delta)]. \tag{42}$$

The Pauli term measures intraband excitations in the conduction band. The general expression for the dynamical susceptibility of an electron gas is

$$\chi(\vec{Q},\omega) = 2\mu_B^2 \sum_{\mathbf{k}} \frac{f(\epsilon_{\vec{k}}) - f(\epsilon_{\vec{k}+\vec{Q}})}{\epsilon_{\vec{k}+\vec{Q}} - \epsilon_{\vec{k}} - (\omega + i\delta)},$$

where $\delta = 0^+$. Taking the imaginary part and letting $\vec{Q}\to 0$ yields

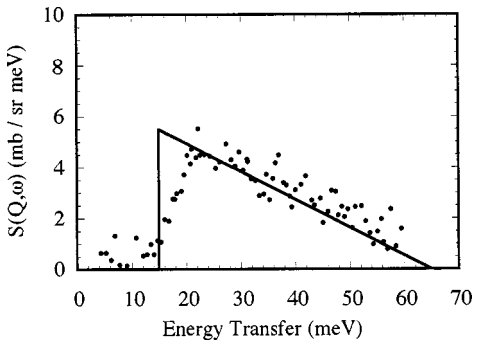

FIG. 1. The energy gap and band density of states as determined by fitting the low temperature inelastic neutron scattering data of Severing *et al.* (Refs. 7,8).

$$\chi''(0,\omega) = \frac{2\pi\mu_B^2}{T}\sum_{\vec{k}} f(\epsilon_{\vec{k}})[1-f(\epsilon_{\vec{k}})]\omega\delta(\omega).$$

The δ function is broadened by the electron life-time, so the final expression for the Pauli contribution to the dynamical susceptibility is

$$\chi''_p(\omega) = \chi_p \frac{\omega\Gamma_e}{\omega^2+\Gamma_e^2}, \tag{43}$$

where χ_p was given in Eq. (35) and Γ_e is the inverse life-time of the band electrons. Finally, the Curie contribution is

$$\chi''_c(\omega) = \chi_c \frac{\omega\Gamma_s}{\omega^2+\Gamma_s^2}, \tag{44}$$

where χ_c was given in Eq. (36) and Γ_s is the inverse of spin-diffusion time. The static susceptibility is related to $\chi''(\vec{Q},\omega)$ by the Kramers-Kronig relation

$$\chi = \frac{1}{\pi}\int_{-\infty}^{\infty}\frac{\chi''(0,\omega)}{\omega}d\omega. \tag{45}$$

It is straightforward to verify that the results in Eqs. (42), (43) and (44) satisfy Eq. (45). This completes the formal part of the theory. In the next section, we compare the theoretical results with experiments.

III. COMPARISON WITH EXPERIMENTS

The zero-temperature limit of $\chi''(0,\omega)$ is the Van Vleck term in Eq. (42)

$$\chi''_{vv}(0,\omega) = 4\pi\mu_{vv}^2 D(\omega-\Delta).$$

Thus, both Δ and $D(\epsilon)$ can be extracted from the low temperature inelastic neutron scattering data as shown in Fig. 1. We have idealized the shape of $D(\epsilon)$ in order to simplify later calculations. The parameters to be used are $\Delta = 180$ K and

$$D(\epsilon) = \frac{2}{W}\left(1-\frac{\epsilon}{W}\right), \tag{46}$$

for $0 < \epsilon < W$ and $D(\epsilon) = 0$ otherwise, $W = 600$ K. Our choice of Δ agrees with that deduced by Reyes,[4] but our W is only one-half as large.

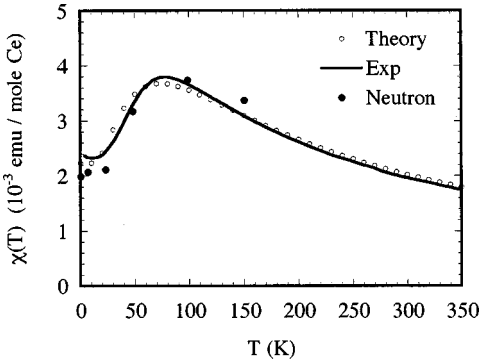

FIG. 2. The calculated temperature dependence of the magnetic susceptibility (open circle) compared with experimental data (solid curve) taken from Ref. 4 and data deduced from neutron scattering (solid circles) (Refs. 7 and 8). The additional fitting parameters are $a_1=0.81, b_1=0.58, \alpha=0.30, \beta=0.91$. The vertical scale is not a fitting parameter.

These parameters are used to calculate the static susceptibility according to Eqs. (34)–(36), and the result is compared with experiments in Fig. 2. Two more parameters are needed, namely $a=0.81$ and $\alpha=0.30$. The paramagnetic moment $1.46\mu_B$ is used for μ_f. The solid circles are data deduced from neutron scattering through the Kramers-Kronig transformation.[7] The overall agreement between theory and experiment is satisfactory, considering the fact that the vertical scale is not a fitting parameter. Notice that $\alpha^2=0.09$ is in the neighborhood of model parameters where the insulating ground state is stable, as discussed in Appendix A. The set of fitting parameters is not unique. A better way to pin down a and α is through the neutron magnetic form factor measurement discussed below.

The neutron magnetic form factor measures separately the f and conduction electron contributions to the susceptibility. The principle of the measurement is discussed in Appendix B. We plot in Fig. 3 the two contributions, χ_d, which is the weight of the conduction-electron form factor, and χ_f, the weight of the f electron form factor. This experiment will help toward refining the model parameters.

In Fig. 4, we compare the calculated specific heat with the result deduced by Kwei *et al.*[6] Both the peak value and its

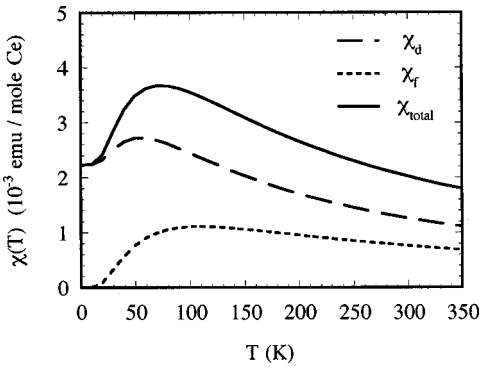

FIG. 3. The d and f components of the magnetic susceptibility, which determine the neutron magnetic form factor. See text and Appendix B. The d component denotes the contribution of the conduction-band electrons. The form factor would help determine the fitting parameter with certainty.

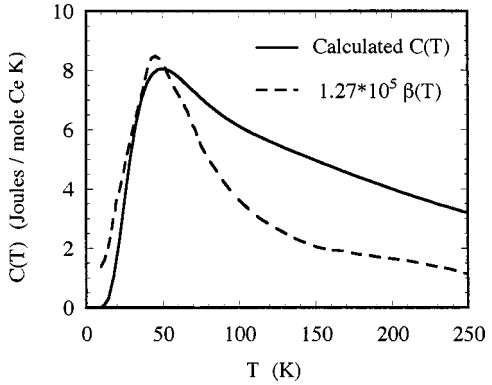

FIG. 4. The calculated electronic specific heat (solid curve) compared with that deduced from anomalous thermal expansion (dashed curve) using the Grüneisen relation (Ref. 6).

position agree with experiment. The entropy under the curve is close to $R\ln 6$, but the number does not originate from the f level degeneracy.

In calculating transport coefficients we encounter one more parameter in the dimensionless quantity

$$\frac{\lambda^2\hbar^2}{8m\epsilon}=A\frac{W^2}{\epsilon}\int_0^W D(\epsilon)\beta f(\epsilon)[1-f(\epsilon)]d\epsilon,$$

where A gathers together a number of material parameters. We estimate from the electron density and bandwidth that $A\simeq 1$, and the result for $A=1$ is shown in Fig. 5. The calculated curves with $0.5\leqslant A\leqslant 2$ are virtually indistinguishable. Selected data points from Ref. 3 are plotted for comparison. The discrepancy at low temperatures is most likely a result of the numerous approximations involved in calculating the Coulomb scattering cross-section and screening length, Eqs. (37) and (38), and we have not been able to improve the agreement by varying the factor A.

As discussed previously, the temperature dependence of the resistivity comes from the inverse screening length λ. It is therefore not feasible to determine the gap from the resistivity data.

In Fig. 6, we compare the calculated Hall mobility with the experiment. The added parameter for this calculation is the impurity concentration, which is chosen as $N_i=2.2\times10^{-4}$ per Ce atom. Again, the agreement is satisfactory.

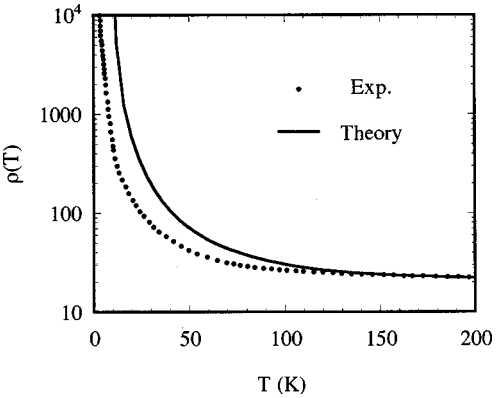

FIG. 5. The calculated electrical resistivity curve (solid curve) compared with selected data points taken from Ref. 3.

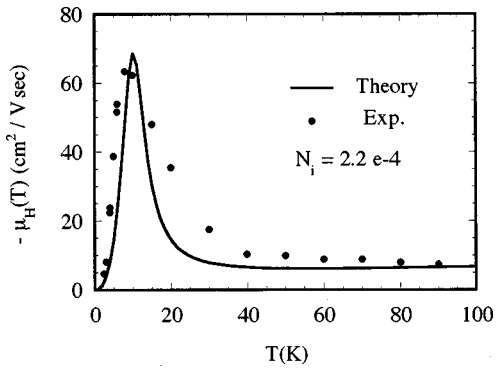

FIG. 6. The calculated Hall mobility (solid curve) compared with data taken from Ref. 3. The density of impurities is measured in units of per Ce atom.

Next, we compare the model prediction for inelastic neutron scattering cross section with the measured results.[7,8] We encounter two more parameters, Γ_e and Γ_s, and there is not enough data to determine them separately. We, therefore, choose $\Gamma_e=\Gamma_s=\Gamma$ and write

$$S(0,\omega)\propto\frac{1}{1-e^{-\beta\omega}}\left[\chi''_{vv}(0,\omega)+(\chi_p+\chi_c)\frac{\omega\Gamma}{\omega^2+\Gamma^2}\right], \tag{47}$$

where $\chi''_{vv}(0,\omega)$ is in Eq. (42). Aside from the vertical scale, the only fitting parameter is Γ, which we choose to be 54 K. For reasons not entirely clear, the predicted scattering intensity in the gap region at high temperatures is somewhat low as shown in Fig. 7. Also, the local state model predicts that the magnetic gap remains the same for all scattering angles. In reality the one- or two-electron impurity states may form

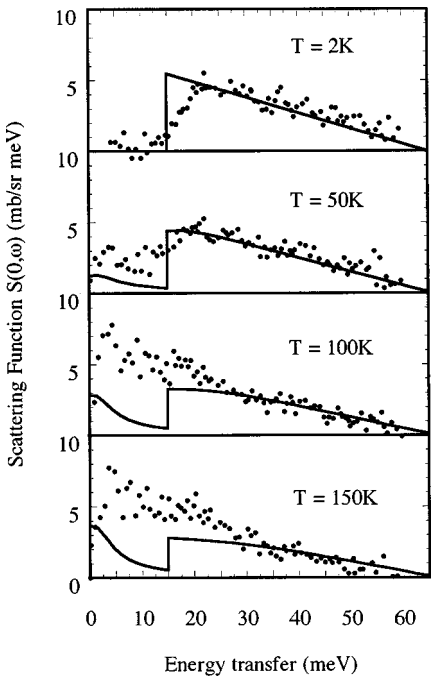

FIG. 7. The calculated inelastic neutron scattering cross section at four different temperatures compared with data from Refs. 7 and 8. The same vertical scale is applied to all theoretical curves.

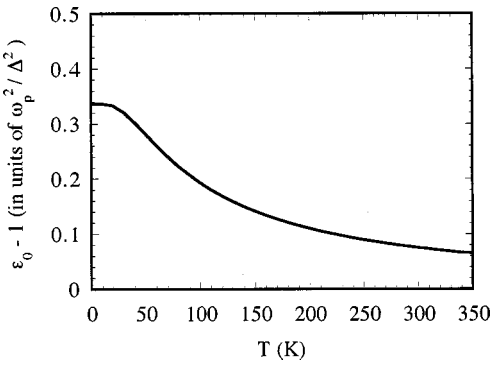

FIG. 8. The predicted polarizability of the material, showing an anomalous increase at low temperatures.

bands. In this case, the range of scattering angle in which the magnetic gap appears would reveal the degree of impurity band dispersion.

The polarizability of a semiconductor is inversely proportional to the square of the energy gap.[23] The material under discussion has a small gap, so we expect a large polarizability or dielectric constant. The formula for the static dielectric constant ϵ_0 is derived by a slight extension of the discussion in Ref. 23

$$\epsilon_0=1+\left(\frac{\omega_p}{\Delta}\right)^2 f(T), \tag{48}$$

where $f(T)$ is a dimensionless function of temperature given by

$$f(T)=\Delta^2\int_0^W\frac{1-n_1-f(\epsilon)}{(\Delta+\epsilon)^2}D(\epsilon)d\epsilon, \tag{49}$$

and ω_p is the plasma frequency given by

$$\omega_p^2=4\pi n_e e^2/m^*.$$

In the last formula n_e is the density of free electrons, one per Ce atom, and m^* is the effective mass. We estimate the ratio $\omega_p^2/\Delta^2\simeq 10^3$ from various material parameters. The plot of $f(T)$ as a function of temperature, Fig. 8, shows that the dielectric constant has a rather large value of 60 at room temperature but rises to 300 at low temperatures. This is another prediction of our theory which can be readily checked experimentally.

We have not tried to fit the temperature dependence of the spin-lattice relaxation rate because the phenomenological band model of Reyes *et al.*, which is very close to ours, gives an adequate account of the data.[4] Also of interest is the observed correlation of lattice parameter with magnetic susceptibility explained by Duan *et al.*[13] The authors showed that one needs to couple the lattice with the magnetic system in order to obtain this effect. Our Fig. 4, which compares the calculated specific heat versus that deduced from anomalous thermal expansion, may be regarded as an alternative way to understand the rapid expansion of the lattice with temperature in the 50–100 K region.

IV. DISCUSSION

As was pointed out in the Introduction, most workers in this field regard the understanding of the narrow conduction

band as the main challenge. It is not the intention of this paper to contradict this common wisdom. Instead, we propose to skip over this difficult step, accept the narrow band as given, and proceed to explore the consequences. The payoff is considerable, because we can account for most of the observed properties of $Ce_3Bi_4Pt_3$. In addition, we suggest neutron scattering as a way to probe this narrow band. In this paper, we assume this band to be *d*. Since the wave-function characteristic of this band enter the neutron magnetic form factor, the low-temperature data would provide a crucial check of this model. If the narrow band is a $d-f$ hybridized band, as is commonly believed, the neutron form factor would show a superposition of both characters at low temperatures. It is our hope that this paper would provide the needed impetus to carried out this experiment on $Ce_3Bi_4Pt_3$ and other *f* electron semiconductors.

ACKNOWLEDGMENTS

The author wishes to thank Professor B. Maple, Professor Z. Fisk, and Professor P. Canfield for their expert guidance through the maze of experimental information, and to thank Professor L. Sham and Professor D. Arovas for informative discussions. He also wishes to acknowledge Professor B. Maple and Professor L. Sham for their hospitality.

APPENDIX A: STABILITY OF THE SEMICONDUCTING STATE

It is difficult to map out the region of parameter space where the semiconducting state is stable because the multidimensional nature of the space. We have only succeeded in finding a neighborhood in the parameter space where the energy gap Δ has the right order of magnitude. The neighborhood itself tell us a considerable amount of the underlying physics.

We introduce two variables x and y such that

$$\epsilon_f-\langle\epsilon\rangle+U_{df}=2V_0\sinh x, \tag{A1}$$

and

$$\epsilon_f-\langle\epsilon\rangle+2U_{df}-U_{dd}=2\sqrt{2}V_0\sinh y. \tag{A2}$$

Both variables quantify the degree of hybridization of the local states. Then, we can write

$$\alpha^2=\frac{1}{4}(1-\tanh y), \tag{A3}$$

which puts $0\leqslant\alpha^2\leqslant 0.5$, and

$$\Delta=-\langle\epsilon\rangle-V_0e^{-x}+\sqrt{2}V_0e^{-y}+(U_{dd}-4V_0\sinh x)\alpha^2. \tag{A4}$$

The hybridization potential $V_0\simeq 0.1$ eV and the Coulomb potential $U_{dd}\simeq 1$ eV. The average band energy $\langle\epsilon\rangle$ is scaled by the bandwidth *W*. For a regular *d* band with $W\simeq 1$ eV, the semiconducting state described in this work cannot be stable because $\Delta<0$. For a narrow band material such as $Ce_3Bi_4Pt_3$ with $W\simeq 0.1$ eV, the semiconducting state with a small gap $\Delta\simeq 0.01$ eV can be stable if $x\simeq 0$ and $\alpha^2\simeq 0.1$ ($y\simeq 0.7$). In this neighborhood both one- and two-electron states are well hybridized.

APPENDIX B: MAGNETIC SUSCEPTIBILITIES AND FORM FACTORS

Consider a system whose ground state $|0\rangle$ is nonmagnetic. An applied magnetic field can induce a paramagnetic response by mixing the ground state with magnetic excited states, resulting in a Van Vleck susceptibility[19]

$$\chi_{vv}=2\sum_m\frac{|\langle 0|M|m\rangle|^2}{E_m-E_0}, \tag{B1}$$

where M is the total magnetic moment operator and E_m is the energy of the eigenstate $|m\rangle$. In the present problem $|0\rangle=\Phi_j^\dagger|\text{vac}\rangle$ and $|m\rangle\equiv|\vec{k}\sigma\rangle=\phi_{j\sigma}^\dagger c_{\vec{k},-\sigma}^\dagger|\text{vac}\rangle$, where $|\text{vac}\rangle$ is the vacuum state. Thus, $E_m-E_0=\Delta+\epsilon_k$. The operator $M=\Sigma_j M_j$, where M_j is the magnetic moment of the jth Ce site

$$M_j=\mu_f(f_{j+}^\dagger f_{j+}-f_{j-}^\dagger f_{j-})+\mu_B(d_{j+}^\dagger d_{j+}-d_{j-}^\dagger d_{j-}), \tag{B2}$$

with the total (local plus band) *d* electron operator given by

$$d_{j\sigma}=c_{j\sigma}+\frac{1}{\sqrt{N}}\sum_{\vec{k}}\tilde{c}_{\vec{k}\sigma}. \tag{B3}$$

We find $\langle 0|M_j|\vec{k}\pm\rangle=\pm e^{-i\vec{k}\cdot\vec{R}_j}\mu_{vv}/\sqrt{N}$, where $\mu_{vv}=b(\alpha+\beta)\mu_B$. The *f* electron makes no contribution. The energy denominator equals $\Delta+\epsilon_k$. Therefore, Eq. (B1) now reads

$$\chi_{vv}=\frac{2\mu_{vv}^2}{N}\sum_{\vec{k}\sigma}\frac{1}{\Delta+\epsilon_k}. \tag{B4}$$

At finite temperatures we insert the appropriate thermal factors to obtain the final formula in Eq. (34).

The effective magnetic moment in the Curie susceptibility term is

$$\mu_c=\langle\phi_{j\sigma}|M_j|\phi_{j\sigma}\rangle=\pm(a^2\mu_f+b^2\mu_B). \tag{B5}$$

This result is used in Eq. (36).

The neutron magnetic form factor measures the Fourier transform of the magnetic moment density of a periodic solid. In a paramagnetic solid the moment is induced by a uniform field, and the neutron magnetic form factor is defined by

$$\chi(\vec{G})=i\int_{-\infty}^{\infty}\langle TM(\vec{G},t)M(0,0)\rangle dt, \tag{B6}$$

where $\vec{G}$ is a reciprocal lattice vector and $M(\vec{G},t)$ is the Heisenberg operator of the Fourier transform of the magnetic moment density $M(\vec{r})$. If we define the tight-binding wave functions of the *f* and conduction electrons by $\phi_f(\vec{r})$ and $\phi_d(\vec{r})$, respectively, then we write

$$M(\vec{G})=\sum_j [\mu_f(f_{j+}^\dagger f_{j+}-f_{j-}^\dagger f_{j-})F_f(\vec{G}) + \mu_B(d_{j+}^\dagger d_{j+}-d_{j-}^\dagger d_{j-})F_d(\vec{G})], \quad \text{(B7)}$$

where

$$F_f(\vec{G})=\int \phi_f^*(\vec{r})e^{i\vec{G}\cdot\vec{r}}\phi_f(\vec{r})d^3r, \quad \text{(B8)}$$

and a similar result for $F_d(\vec{G})$. The final result shows that

$$\chi(\vec{G})=F_d(\vec{G})\chi_d+F_f(\vec{G})\chi_f, \quad \text{(B9)}$$

where

$$\chi_d=\chi_{vv}+\chi_p+\frac{b^2\mu_B}{\mu_c}\chi_c, \quad \text{(B10)}$$

and

$$\chi_f=\frac{a^2\mu_f}{\mu_c}\chi_c. \quad \text{(B11)}$$

The components χ_d and χ_f are plotted in Fig. 3.

[1] Z. Fisk *et al.*, Physica B **206&207**, 798 (1995), and references cited therein.
[2] M. F. Hundley, P. C. Canfield, J. D. Thompson, Z. Fisk, and J. M. Lawrence, Phys. Rev. B **42**, 6842 (1992).
[3] Z. Fisk, P. C. Canfield, J. D. Thompson, and M. F. Hundley, J. Alloys Compd. **181**, 369 (1992).
[4] A. P. Reyes, R. H. Heffner, P. C. Canfield, J. D. Thompson, and Z. Fisk, Phys. Rev. B **49**, 16 321 (1994).
[5] P. C. Canfield, J. D. Thompson, Z. Fisk, M. F. Hundley, and A. Lacerda, J. Magn. Magn. Mater. **108**, 217 (1992).
[6] G. H. Kwei, J. M. Lawrence, P. C. Canfield, W. P. Beyermann, J. D. Thompson, Z. Fisk, A. C. Lawson, and J. A. Goldstone, Phys. Rev. B **46**, 8067 (1992).
[7] A. Severing, J. D. Thompson, P. C. Canfield, Z. Fisk, and P. Riseborough, Phys. Rev. B **44**, 6832 (1991).
[8] A. Severing, J. D. Thompson, P. C. Canfield, Z. Fisk, and P. Riseborough, J. Alloys Compd. **181**, 211 (1992).
[9] P. C. Canfield, J. D. Thompson, Z. Fisk, M. F. Hundley, and A. Lacerda, J. Magn. Magn. Mater. **108**, 217 (1992).
[10] S. Kondo *et al.*, Phys. Rev. Lett. **78**, 3279 (1997).
[11] A. Auerbach and K. Levin, Phys. Rev. Lett. **57**, 877 (1986); Phys. Rev. B **34**, 3524 (1986).
[12] A. J. Millis and P. A. Lee, Phys. Rev. B **35**, 3394 (1987).
[13] J.-M. Duan, D. P. Arovas, and L. J. Sham, Phys. Rev. Lett. **79**, 2097 (1997).
[14] T. Portengen, Th. Ostreich, and L. J. Sham, Phys. Rev. Lett. **76**, 3384 (1996).
[15] T. Portengen, Th. Ostreich, and L. J. Sham, Phys. Rev. B **54**, 17 452 (1996).
[16] L. M. Falicov and J. C. Kimball, Phys. Rev. Lett. **22**, 997 (1968).
[17] R. Ramirez, L. M. Falicov, and J. C. Kimball, Phys. Rev. B **2**, 3383 (1970).
[18] S. H. Liu, Phys. Rev. Lett. **58**, 2706 (1987); Phys. Rev. B **37**, 3542 (1988); Physica B **240**, 49 (1997).
[19] J. M. Ziman, *Principles of the Theory of Solids* (Cambridge University Press, Cambridge, England, 1964), Chap. 10, p. 284.
[20] J. M. Ziman, *Principles of the Theory of Solids* (Ref. 19), Chap. 7, p. 188.
[21] J. M. Ziman, *Principles of the Theory of Solids* (Ref. 19), Chap. 5, p. 129.
[22] A. J. Dekker, *Solid State Physics* (Prentice Hall, Englewood Cliffs, NJ, 1957), Chap. 13, pp. 326–328.
[23] J. M. Ziman, *Solid State Physics* (Ref. 22), Chap. 5, p. 139.